corrected, a photon is emitted incoherently into the environment, destroying quantum coherence for the unit from which it was emitted. In contrast to the switching of bits with π pulses, in which photons are emitted and absorbed coherently, the correction of errors with the use of fast decays is inherently dissipative.

Arrays of pulsed, weakly coupled quantum systems provide a potentially realizable basis for quantum computation. The basic unit in the array could be a quantum dot, a nuclear spin, a localized electronic state in a polymer, or any multistate quantum system that interacts locally with its neighbors and can be compelled to switch between states with resonant pulses of light. Many variations on the scheme presented here exist: The arrays could be two- or three-dimensional, for example, or the switching process could take place through intermediate states with the use of multiple pulses (*14*). The primary technical problems in the construction and operation of such a computer are the identification of man-made or natural systems with appropriate long-lived localized states and the delivery of the proper sequence of accurate pulses. If they can be built, the devices will combine digital and quantum analog capacities to allow the creation and manipulation of complicated many-bit quantum states and to probe the limits set by the fundamental physics of computation.

REFERENCES AND NOTES

1. R. Landauer, *IBM J. Res. Dev.* **5**, 183 (1961).
2. K. K. Likharev, *Int. J. Theor. Phys.* **21**, 311 (1982).
3. C. H. Bennett, *IBM J. Res. Dev.* **17**, 525 (1973); *Int. J. Theor. Phys.* **21**, 905 (1982). Y. Lecerf, *Compte Rendus* **257**, 2597 (1963); *ibid.*, p. 2940.
4. E. Fredkin and T. Toffoli, *Int. J. Theor. Phys.* **21**, 219 (1982).
5. P. Benioff, *J. Stat. Phys.* **22**, 563 (1980); *Phys. Rev. Lett.* **48**, 1581 (1982); *J. Stat. Phys.* **29**, 515 (1982); *Ann. N.Y. Acad. Sci.* **480**, 475 (1986).
6. D. Deutsch, *Proc. R. Soc. London Ser. A* **400**, 97 (1985); *ibid.* **425**, 73 (1989).
7. R. P. Feynman, *Opt. News* **11**, 11 (1985); *Found. Phys.* **16**, 507 (1986); *Int. J. Theor. Phys.* **21**, 467 (1982).
8. W. H. Zurek, *Phys. Rev. Lett.* **53**, 391 (1984).
9. A. Peres, *Phys. Rev. A* **32**, 3266 (1985).
10. N. Margolus, *Ann. N.Y. Acad. Sci.* **480**, 487 (1986); in *Complexity, Entropy, and the Physics of Information*, W. H. Zurek, Ed. (Sante Fe Institute Series, vol. 8, Addison Wesley, Redwood City, CA 1991), pp. 273–288.
11. F. L. Carter, *Molecular Electronics* (Dekker, New York, 1982); *Molecular Electronics II* (Dekker, New York, 1987).
12. D. K. Ferry, J. R. Barker, C. Jacobini, *Granular Nanoelectronics* (Plenum, New York, 1991); K. E. Drexler, *Nanosystems* (Wiley, New York, 1992); see also the now defunct *J. Mol. Electron.*
13. J. J. Hopfield, J. N. Onuchic, D. N. Beratan, *Science* **241**, 817 (1988).
14. K. Obermayer, W. G. Teich, G. Mahler, *Phys. Rev. B* **37**, 8096 (1988); W. G. Teich, K. Obermayer, G. Mahler, *ibid.*, p. 8111; W. G. Teich and G. Mahler, *Phys. Rev. A* **45**, 3300 (1992).
15. L. Allen and J. H. Eberly, *Optical Resonance and Two-Level Atoms* (Wiley, New York, 1975).
16. W. H. Louisell, *Quantum Statistical Properties of Radiation* (Wiley, New York, 1973).
17. S. Wolfram, *Rev. Mod. Phys.* **55**, 601 (1983).
18. A. Einstein, B. Podolsky, N. Rosen, *Phys. Rev.* **47**, 777 (1935).
19. J. P. Paz and G. Mahler, in preparation.
20. S. Lloyd, *Programming Pulsed Quantum Computers*, in preparation.

19 April 1993; accepted 19 July 1993

A UV-Sensitive Mutant of *Arabidopsis* Defective in the Repair of Pyrimidine-Pyrimidinone(6-4) Dimers

A. B. Britt,* J.-J. Chen, D. Wykoff, D. Mitchell

Plants are continually subjected to ultraviolet-B (UV-B) irradiation (290 to 320 nanometers) as a component of sunlight, which induces a variety of types of damage to the plant DNA. Repair of the two major DNA photoproducts was analyzed in wild-type *Arabidopsis thaliana* and in a mutant derivative whose growth was sensitive to UV-B radiation. In wild-type seedlings, repair of cyclobutane pyrimidine dimers occurred more slowly in the dark than in the light; repair of this photoproduct was not affected in the mutant. Repair, in the dark, of pyrimidine-pyrimidinone(6-4) dimers was defective in the UV-sensitive mutant.

The developmental strategy of plants differs from that of animals in a way that enhances the beneficial effects of random mutagenesis and diminishes its harmful effects (*1*, *2*). Although progress has been made in the genetics and biochemistry of repair in the single-cell green alga *Chlamydomonas* (*3*), studies of DNA repair in higher plants have been relatively limited (*4*). Many early studies presented negative results that led to the suggestion that DNA repair does not occur in plants. Both photorepair and excision repair of UV-induced photoproducts have been demonstrated in phytoplankton (*5*) and in several higher plants (*6*). A cyclobutane pyrimidine dimer photolyase activity has been observed in *Arabidopsis thaliana* (*7*).

A complete understanding of the various repair pathways in plants requires an integrated biochemical, molecular, and genetic approach. There has been, to our knowledge, no report of a mutant in any higher plant that is specifically defective in DNA repair, so we initiated a search for DNA repair mutants of *Arabidopsis*. To increase the penetration of UV light through the plant tissue, we used plants homozygous for the mutation *tt5* [*transparent testa* (*8*)] for all experiments. This stock is derived from the Landsberg *erecta* ecotype and is defective in the production of UV-absorbing flavonoid pigments. We mutagenized seeds (termed the M1 or primary mutagenized population) by soaking them in 0.3% ethylmethane sulfonate (EMS), then grew them to maturity, allowed them to self-pollinate, and harvested them in bulk. The seeds resulting from the self-pollination of the M1 plants, termed the M2 population, carry EMS-induced mutations in either the heterozygous or homozygous state. The M2 seeds were sown and self-pollinated, and the mature plants were harvested individually to yield M2 "families." Any M2 plant that is homozygous for a mutation will produce, after self-pollination, a family of progeny in which every individual is homozygous for that mutation. A sample of seeds from each M2 family was tested for sensitivity to UV by analysis of root growth after exposure to UV light.

Approximately 20 seeds from each M2 family were placed on a nutritive agar plate (*9*) and incubated at 22°C under light filtered through orange polyvinyl chloride [photosynthetically active radiation (PAR) was equal to 5 μmol/m^2·s]. Plates were incubated on edge (vertically), and the roots of the seedlings grew downward across the surface of the agar. After 3 days, half of each row of seedlings was exposed to 0.5 kJ/m^2 of UV-B from a UV transilluminator. After irradiation, the plates were rotated by 90° and incubated overnight in complete darkness. Because the plate was rotated, any new growth (after UV-B irradiation) was at right angles to the old growth. Families made up of seedlings that continued to grow on the unirradiated side of the plate but failed to grow on the irradiated side were scored as UV-sensitive (Fig. 1A). Families that uniformly expressed a UV-sensitive phenotype were propagated and backcrossed to their progenitor.

Two UV-sensitive families were detected in a screen of over 2000 mutagenized families. The UV-sensitive phenotype in both of these isolates segregated as a single recessive mutation located approximately

A. B. Britt, J.-J. Chen, D. Wykoff, Section of Botany, University of California at Davis, Davis, CA 95616.
D. Mitchell, Department of Carcinogenesis, The University of Texas M. D. Anderson Cancer Research Center, Smithville, TX 78957.

*To whom correspondence should be addressed.

27 map units away from the *tt5* locus (Table 1). Because the F_1 progeny that resulted from crosses between these lines uniformly displayed a UV-sensitive phenotype, both mutants carry a mutation in the same gene, and therefore one UV-sensitive line is probably a re-isolate of the other. For this reason, only a single UV-sensitive mutant line, designated *uvr1*, was further characterized. Additional crosses to a tester [*hy2* (*long hypocotyl*), *gl1* (*glabra*), *tt5*] line placed the *uvr1* locus at 45.9 ± 1.3 centimorgans (cM) on the map of Koornneef *et al.* (*10*), between the wild-type *GL1* and *TT5* loci (Table 1).

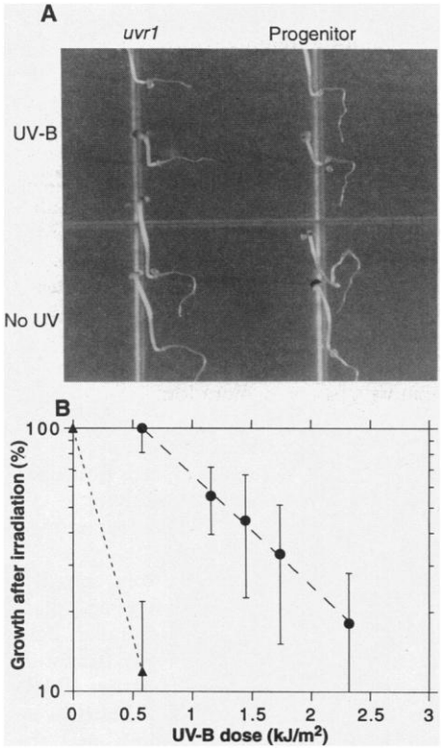

Fig. 1. (**A**) M2 families uniformly homozygous for UV sensitivity were identified with a root-bending assay. Each row of seedlings was exposed to 0.5 kJ/m^2 of UV-B [measured with a UV-B radiometer (UVP, San Gabriel, California)] from a UV transilluminator (Fisher, Pittsburgh, Pennsylvania) with a peak output at 305 nm, filtered through a 0.005-ml cellulose acetate sheet that absorbed the UV-C fraction of the emitted light. Total exposure time was approximately 40 s. After irradiation, the plates were rotated by 90°. (**B**) Inhibition of root growth in the *uvr1* strain (triangles) and its progenitor (circles). New root growth (at right angles to the growth before irradiation) was measured 3 days after irradiation at the indicated UV-B doses. After irradiation, seedlings were grown at 22°C in the dark. The growth of *Arabidopsis* seedlings, under these conditions, ceases by the sixth day after imbibition. The results represent an average of measurements made on between 10 and 31 seedlings. Error bars are 1 SD.

The *uvr1* mutant was approximately sixfold more sensitive than its progenitor to the inhibitory effects of UV-B on elongation of the immature root (Fig. 1B). Not only was the growth of the root tip sensitive to UV-B irradiation, but the aerial tissues of the plant also displayed a UV-sensitive phenotype. Cool white fluorescent lamps emit a minor fraction of their power (approximately 0.04 W/m^2 at the level of the soil) as a small peak at 313 nm (*11*). The harvested stems of the mutant line were blackened on their illuminated surface, in distinct contrast to the bright yellow color of their *tt5* progenitor. Most notably, the leaves of the mutant gradually turned brown and withered, and the edges curled upward and inward to form a concave bowl. This curling indicates that cell growth is inhibited on the upper (irradiated) surface of the leaf. In contrast, the phenotype of the *uvr1* mutant grown under the light of cool white lamps filtered through Mylar, which blocks the UV-B component of the lamp's output, was very similar to that of the *tt5* progenitor.

We assayed the induction of cyclobutane pyrimidine dimers (CPDs), the most common UV-induced DNA photoproduct, in *uvr1* and progenitor 5-day-old seedlings. We assayed the concentration of CPDs by comparing the weight-average molecular weights of single-stranded DNA (assayed by alkaline sucrose gradient sedimentation) in samples treated with an endonuclease specific to CPDs (T4 UV-endonuclease V) with that of the same DNA sample that had not been subjected to digestion. The concentration of CPDs immediately after irradiation was the same in the mutant and progenitor lines (Fig. 2). Hence, the seedlings were identical in their transparency to UV-B.

We measured the rate of loss of the two major photoproducts induced by UV: the CPD and the pyrimidine-pyrimidinone(6-4) dimer [(6-4) photoproduct]. Seeds of the *uvr1* and progenitor lines were grown on nutritive agar plates (9) plus 0.5% sucrose and incubated on edge under continuous low light (as described above) for 5 days. The seedlings were then irradiated with UV-B light (Fig. 1) and received a dose of 1.25 kJ/m^2 over a period of 40 s. The seedlings were then either immediately harvested (in the dark) for DNA extraction, further incubated in complete darkness for dark repair assays, or incubated under fluorescent lamps for a period of 1 to 20 hours for photoreactivation studies. The concentrations of CPDs and (6-4) photoproducts were assayed with the use of a lesion-specific radioimmunoassay (*12*).

Both the wild-type and *uvr1* strains repaired CPDs inefficiently, if at all, in the dark and photoreactivated CPDs rapidly (Fig. 3A). The results for the progenitor strain are in good agreement with those previously obtained with T4 endonuclease V–alkaline sucrose gradient analysis (*7*). The ability of the wild-type *Arabidopsis* line to continue to grow normally (Fig. 1B) in spite of the persistence of CPDs at a frequency of approximately one dimer per 42,000 bases (Fig. 2) suggests that *Arabidopsis* has some capacity to tolerate this type of dimer. It is also possible that selective, rapid repair occurs at a small subclass of critical sites, such as within actively transcribed genes. Site-specific repair of critical regions has been observed in mammalian systems (*13, 14*) and has been suggested as the means by which rodent cell lines tolerate the persistence of a relatively high overall frequency of CPDs.

Although much attention has been focused on the repair of CPDs, the (6-4) photoproduct has been increasingly implicated both as a significant source of cytotoxicity in mammalian tissues and as an important premutagenic lesion in *Escherichia coli* (*15–17*). The importance of this relatively minor photoproduct in UV cytotoxicity is underscored by the repair phenotypes of certain mutant mammalian cell lines. Although most UV-sensitive cell

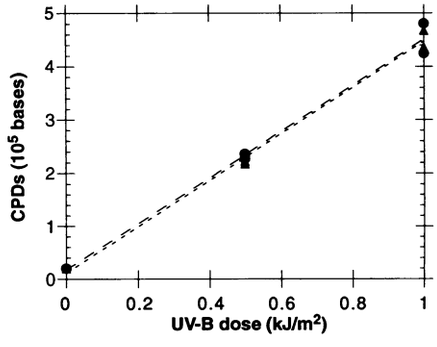

Fig. 2. Cyclobutane pyrimidine dimers are induced at equal rates in the *uvr1* mutant (triangles) and its progenitor (circles). Seedlings were grown on vertically oriented nutrient agar plates plus 0.5% sucrose. Approximately 500 to 1000 seeds were sown per 100 mm by 100 mm plate. To label the DNA, we also included [^{3}H]thymidine (1 μCi/ml) in the medium. Five-day-old seedlings were irradiated under the UV-B source described in Fig. 1 for 20 to 40 s to produce the final UV-B dose. The DNA was then immediately extracted (*29*). The CPDs were assayed by digestion with T4 endonuclease V and sized with an alkaline sucrose gradient (*30*). The number of CPDs per base was calculated as $1/x_E = 1/x_D - 1/x_U$, where x_E is the average length (based on the weight-average molecular weight) in bases between enzyme-sensitive sites, x_D is the average length of the digested DNA sample, and x_U is the average length of the undigested sample.

lines are defective in the repair of both (6-4) photoproducts and CPDs, certain mutant lines, including some UV-resistant revertant lines (*18*), are defective only in the repair of CPDs. The relatively UV resistant and, in some cases, antimutator (*19*) phenotype of these lines suggests that (6-4) products function as cytotoxic lesions in animal tissues (*20*).

In the dark, repair of the (6-4) photoproduct occurs much faster than repair of CPDs in our progenitor line, with approximately 50% of the initial lesions eliminated within the first 2 hours after irradiation (Fig. 3B). *Arabidopsis* therefore resembles other biological systems, including fish, frog, and rodent cells (*15*), in that the rate of repair, in the dark, of CPDs is low or undetectable, whereas (6-4) photoproducts are rapidly removed. In contrast, little or no repair of (6-4) photoproducts occurs in *uvr1* mutant plants (Fig. 3B). The sensitivity of this strain to low levels of UV-B suggests that repair of this lesion is essential for resistance to environmental UV-B. In addition, it is possible that the *uvr1* gene is required for the repair of other UV-induced photoproducts, such as pyrimidine hydrates, and that the persistence of these other lesions may contribute significantly to the UV-sensitive phenotype of the *uvr1* mutant. It may also be possible that *Arabidopsis*, like mammalian cells, is capable of rapid removal of CPDs from a minor but critical subclass of sites and that the *uvr1* gene is also required for this process.

In *E. coli*, both the (6-4) photoproduct and the CPD are repaired by a single excision repair holoenzyme, the UvrABC endonuclease (*21*, *22*). This enzyme recognizes a wide variety of DNA damage products and facilitates their repair by specifically nicking the damaged DNA strand. In contrast, reversion of CPDs by the *E. coli* photolyase is specific for CPDs (*23*). The mechanistic relation between overall repair of CPDs, site-specific repair of CPDs, and repair of (6-4) photoproducts in higher animal systems is more complex. The greater efficiency of (6-4) photoproduct repair compared to that of CPD repair is generally thought to reflect a higher affinity of the repair complex for the (6-4) photoproduct. It is possible, however, that some genes are required for the excision of many types of DNA damage products, whereas others are specific for a single type of lesion. Because dark repair of CPDs is slow in *Arabidopsis*, we cannot conclude from the data presented here whether the *uvr1* mutant, which is clearly defective in the repair of (6-4) products, might also be defective in the excision repair of CPDs.

It is conceivable that the *uvr1* mutant is UV-sensitive for some reason other than a defect in DNA repair and that its failure to repair (6-4) photoproducts after UV irradiation is, like its failure to grow after UV irradiation, the result, rather than the cause, of its UV sensitivity. The fact that the mutant efficiently photorepairs CPDs at the wild-type rate, however, makes this possibility unlikely and suggests that the *uvr1* mutation is in a gene specifically required for DNA repair.

The generation and characterization of DNA repair mutants, most notably in *E. coli*, has elucidated the regulation, variety, and biological importance of the many pathways involved in DNA repair. Because of its small physical size (and hence UV transparency), small genome, efficiency of mutagenesis, and short generation time, *Arabidopsis thaliana* is well suited as a model system for the study of the molecular genetics of DNA repair in higher plants. Recent awareness of the increasing degradation of the UV-B–absorbing ozone layer (*24*, *25*) has focused attention

Table 1. Segregation analysis of *uvr1* indicates that it is a single recessive mutation located between *GL1* and *TT5* on chromosome 3. The UV-sensitive phenotype of individual F_2 plants was determined by a root sensitivity assay of 12 or more F_3 progeny. Linkage to *GL1* was determined from F_3 segregation data as described by Koornneef *et al.* (*10*). Linkage to *HY2* (in repulsion) and *tt5* (in coupling) was determined from the entire F_2 population by the maximum likelihood method (*27*), and the standard deviation was derived as described by Allard (*28*). The recombination percentages (and their standard deviations) were converted to map units (that is, corrected for multiple crossovers) with the Kosambi mapping function (*10*). The χ^2 values in column 4 represent the fit of the data to a 3:1 segregation ratio for *uvr1*; the χ^2 values in column 5 represent the fit of the data to the derived recombination rates. The genetic markers are located at 0 (*HY2*), 39.6 (*GL1*), and 77.8 (*TT5*) cM on chromosome 3. Blank spaces indicate data not determined.

F_1 cross	F_2 segregation		UV-sensitive F_2 progeny (%)	Map distance ± SD (cM)
	Phenotypes	*n*		
uvr1, *tt5* (first isolate)	UVR1/-, TT5/-	152	21.4	28.2 ± 4.7
× *UVR1*, *TT5*	UVR1/-, tt5	28	χ^2 = 1.585	χ^2 = 1.71
	uvr1, TT5/-	21		
	uvr1, tt5	28		
uvr1, *tt5* (second isolate)	UVR1/-, TT5/-	54	24.7	30.8 ± 8.3
× *UVR1*, *TT5*	UVR1/-, tt5	10	χ^2 = 0.004	χ^2 = 0.004
	uvr1, TT5/-	10		
	uvr1, tt5	11		
HY2, *GL1*, *uvr1*	GL1/-, UVR1/-	94	29.8	
× *hy2*, *gl1*, *UVR1*	gl1, UVR1/-	45	χ^2 = 2.431	
	GL1/-, uvr1*	59		6.3 ± 1.3*
	gl1, uvr1	0		χ^2 = 2.75
	HY2/-, UVR1/-	100		48.2 ± 13.6
	hy2, UVR1/-	39		χ^2 = 2.47
	HY2/-, uvr1	51		
	hy2, uvr1	8		

*The genotypes of these F_2 plants were identified in the F_3 segregation as *GL1/GL1*, *uvr1/uvr1* (*n* = 52) and *GL1/gl1*, *uvr1/uvr1* (*n* = 7). The map distance is based on this F_3 segregation.

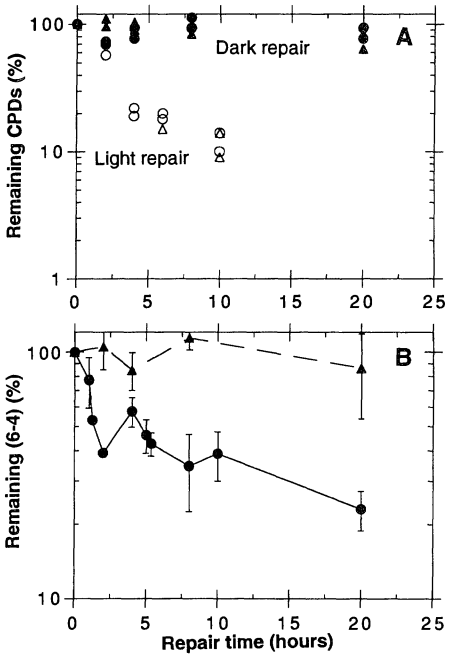

Fig. 3. (**A**) Repair of CPDs is similar in both the *uvr1* (triangles) and progenitor (circles) strains. Solid symbols indicate dark repair; open symbols, light repair. Seedlings were grown on agar plates and irradiated to a final UV-B dose of 1.32 J/m^2 as described (Fig. 2). The *uvr1* seedlings are derived from a backcrossed line. Photoreactivation was carried out under a bank of General Electric Cool White fluorescent lamps whose light was filtered through the polystyrene lid of the petri dish. The UV-A flux at the surface of the agar was approximately 0.08 W/m^2 [measured with a UV-A radiometer (UVP)]. (**B**) The *uvr1* mutant is defective in the repair of the (6-4) product. After irradiation, seedlings were incubated at 22°C in the dark. The data represent an average of two to eight experimental values; error bars are 1 SD.

on the mechanisms of UV-B resistance in plants (*26*). UV-B intensity also varies widely with season, latitude, and altitude. Like resistance to other environmental stresses such as drought or cold, the degree of tolerance of a particular plant species to UV-B may influence the range of environments at which certain plant species can survive. We have shown that the ability to efficiently repair (6-4) photoproducts is an essential component of UV-B resistance in *Arabidopsis*.

REFERENCES AND NOTES

1. V. Walbot, *Trends Genet.* 1, 165 (1985).
2. E. J. Klekowski, *Mutation, Developmental Selection, and Plant Evolution* (Columbia Univ. Press, New York, 1988).
3. G. D. Small, *Mutat. Res.* **181**, 31 (1987).
4. J. Veleminsky and K. Angelis, in *Mutation and the Environment*, R. Mortimer, L. Mendelsohn, R. Albertini, Eds. (Wiley-Liss, New York, 1990), vol. 340, pp. 195–203.
5. D. Karentz, J. E. Cleaver, D. L. Mitchell, *J. Phycol.* **27**, 326 (1991).
6. A. G. McLennan, *Mutat. Res.* **181**, 1 (1987).
7. Q. Pang and J. B. Hays, *Plant Physiol.* **95**, 536 (1991).
8. M. Koornneff, Arabidopsis *Inf. Serv.* **27**, 1 (1990).
9. A. R. Kranz and B. Kirchheim, in *Genetic Resources in* Arabidopsis, A. R. Kranz, Ed. (*Arabidopsis* Information Service, Botanical Institute, J. W. Goethe-University, Frankfurt, 1987), vol. 24, p. 421.
10. M. Koornneef *et al.*, *J. Hered.* **74**, 265 (1983).
11. *ISCO Tables* (Instrumentation Specialties Company, Lincoln, NE, 1970).
12. D. L. Mitchell, C. A. Haipek, J. M. Clarkson, *Mutat. Res.* **143**, 109 (1985).
13. V. A. Bohr, C. A. Smith, D. S. Okumoto, P. C. Hanawalt, *Cell* **40**, 359 (1985).
14. D. C. Thomas, D. S. Okumoto, A. Sancar, V. A. Bohr, *J. Biol. Chem.* **264**, 18005 (1989).
15. D. L. Mitchell and R. S. Nairn, *Photochem. Photobiol.* **49**, 805 (1989).
16. W. A. Franklin and W. A. Haseltine, *Mutat. Res.* **165**, 1 (1986).
17. D. E. Brash and W. A. Haseltine, *Nature* **298**, 189 (1982).
18. J. E. Cleaver *et al.*, *Mol. Cell. Biol.* **7**, 3353 (1987).
19. M. Z. Zdzienicka *et al.*, *Mutat. Res.* **273**, 73 (1992).
20. L. H. Thompson *et al.*, *Mutagenesis* **4**, 140 (1989).
21. W. A. Franklin and W. A. Haseltine, *Proc. Natl. Acad. Sci. U.S.A.* **81**, 3821 (1984).
22. A. Sancar and W. D. Rupp, *Cell* **33**, 249 (1983).
23. D. E. Brash, W. A. Franklin, G. B. Sancar, A. Sancar, W. A. Haseltine, *J. Biol. Chem.* **260**, 11438 (1985).
24. J. E. Frederick and D. Lubin, *Photochem. Photobiol.* **47**, 571 (1988).
25. F. E. Quaite, B. M. Sutherland, J. C. Sutherland, *Nature* **358**, 576 (1992).
26. A. Stapleton, *Plant Cell* **4**, 1353 (1992).
27. R. A. Fisher and B. Balmukand, *J. Genet.* **20**, 79 (1928).
28. R. W. Allard, *Hilgardia* **24**, 235 (1956).
29. M. Shure, S. Wessler, N. Fedoroff, *Cell* **35**, 225 (1983).
30. A. K. Ganesan, C. A. Smith, A. A. van Zeeland, in *DNA Repair*, E. C. Freidberg and P. C. Hanawalt, Eds. (Dekker, New York, 1981), vol. 1A, pp. 89–98.

31. The authors thank T. Murphy, A. Smith, and M. Learned for their valuable advice and encouragement. We also thank A. Ganesan for the T4 endonuclease V and A. Lloyd and M. Koornneef for supplying mutants of *Arabidopsis*. Supported by grant DMB-90-19159 from the NSF, Division of Molecular Biosciences.

22 March 1993; accepted 30 July 1993

Major Groove Accessibility of RNA

Kevin M. Weeks* and Donald M. Crothers

Chemical acylation experiments showed that the RNA major groove, often assumed to be too deep and narrow to permit recognition interactions, is accessible at duplex termini. Reactivity extended further into the helix in the 5′ than in the 3′ direction. Asymmetric and large loops between helices uncoupled them, which yielded both enhanced reactivity at terminal base pairs and weaker stabilization enthalpy compared to that in small loops or symmetric loops of the same size. Uncoupled helices have effective helix ends with accessible major grooves; such motifs are attractive contributors to protein recognition, tertiary folding, and catalysis.

The geometry of the RNA helix determines, in part, the recognizability of the major and minor grooves (*1*). In a continuous A-form RNA helix, the minor groove is wide and shallow, which facilitates the interaction of base functional groups with complementary ligands. In contrast, the major groove is deep and narrow and may be inaccessible for specific recognition. This fundamental consequence of RNA geometry presents a paradox: the inaccessible major groove presents a richer ensemble of arrayed hydrogen bond acceptors and donors than the minor groove does (*2*). Given the ubiquity of helical segments in RNA and the limits imposed by having only four constituent subunits, many distinguishing interaction surfaces are potentially buried in the major groove.

Despite this prediction, there are several well-characterized examples of RNA recognition achieved by way of interaction in the major groove. The tertiary folding of transfer RNA (tRNA) uses base triplets in which a third nucleotide forms hydrogen bonds with a Watson-Crick base pair in the major groove of short helices (*3*); the guanosine binding site in the *Tetrahymena* ribozyme is located in the major groove at the end of a short, bulged helix (*4*); the yeast aspartyl-tRNA synthetase contacts both the acceptor and anticodon stems from the major groove side (*5*); and peptide models for the RNA binding domain of the human immunodeficiency virus (HIV) Tat protein bind TAR RNA at the major groove adjacent to a bulge loop (*6*, *7*). Major groove inaccessibility is a consequence of the close approach of the phosphoribose backbones for helices of six or more base pairs (bp) (*8*). Accessibility in the major groove might be modulated where this regularity is interrupted.

Diethyl pyrocarbonate (DEPC) carbethoxylates purines primarily at the N7 position in a reaction sensitive to the solvent exposure of the base (*6*, *9*). DEPC has an effective diameter of ~3.5 Å (*10*), which is similar to the width of the deep RNA major groove (~4 Å). DEPC is comparable in size to amino acid and nucleotide motifs that mediate RNA-protein or RNA-RNA interactions; hence, the reactivity rates of this probe reflect the steric accessibility and thus the recognizability of individual purine nucleotides.

Our experiments establish a correlation between DEPC reactivity, which reflects accessibility of the major groove, and the presence of either true or effective helix ends. Effective ends result when adjacent helices are separated by loops that decouple them thermodynamically, as reflected in a diminished enthalpy of melting. We find, in agreement with Peritz *et al.* (*11*), that asymmetric loops are more effective than symmetric loops in lowering overall thermal stability and show that major groove accessibility is relatively enhanced at helix ends that flank asymmetric (and large) loops. These structures constitute an RNA motif capable of specific interaction in the major groove.

RNA duplexes that incorporate simple bulge and internal loops were generated by pairwise combination of 10 synthetic oligoribonucleotides (Fig. 1) (*12*). Duplexes were designed to simplify the experimental protocol and feature a homopurine strand uniquely susceptible to attack by DEPC. All helices include 20 bp and predominantly adenosine bases, which are more reactive toward DEPC (*9*), and include terminal and internal G-C base pairs to prevent fraying and ensure proper duplex register, respectively. Helices are identified by the number of unpaired or mismatched cytosine nucleotides in the center of the duplex. For example, the perfect 20-bp duplex is identified as [00], whereas a dinucleotide bulge on the right hand (pyrimidine) strand is [02] (Fig. 1).

In the absence of complementary oligonucleotides, the 10 single strands (Fig.

Department of Chemistry, Yale University, New Haven, CT 06511.

*Present address: University of Colorado, Department of Chemistry and Biochemistry, Boulder, CO 80309.